FULLY-REVERSED FATIGUE BEHAVIOR OF SCARF JOINT REPAIRS FOR WIND TURBINE BLADE SHELL APPLICATIONS

Carineh Ghafafian[a], Volker Trappe[a]

a: Bundesanstalt für Materialforschung und -prüfung (BAM) – carineh.ghafafan@bam.de

Abstract: *To enable a quick and cost-effective return to service for wind turbine blades, localized repairs can be executed by technicians in the field. Scarf repairs, shown to be highly efficient with a smooth load transition across angled joint walls and a restored aerodynamic profile, are the focus of this work. The failure mechanisms of these structures were examined under quasi-static tensile and fully-reversed cyclic loading. While the scarf ratio was held constant at 1:50, the repair layup was varied between large-to-small and small-to-large. The effect of the presence of resin pockets and the fiber orientation mismatch between parent and repair material on the restored strength of BIAX ±45° glass fiber reinforced polymer scarf joint structures was studied.*

Keywords: glass fiber reinforced polymers; scarf repairs; fatigue

1. Introduction

Composite repairs are commonly done as adhesively bonded joints because of the efficiency in comparison to mechanical joints in terms of a large area over which load is distributed. These structures are especially advantageous as joints in fiber reinforced polymers (FRP), since they avoid drilling holes for fasteners or bolts, which could disrupt load-carrying fibers and create stress concentrations [1]. As the focus of this work, scarf repairs have been shown to be the most efficient in terms of property restoration for composites, and are well-suited for smooth aerodynamic surface repair applications. Angled parent walls are removed, upon which repair layers are attached to create a bond in a thin layer over a large joint area, allowing for more uniform stress distribution of the applied loads for an overall efficient repair [3-6].

70-80% of defects in wind turbine blade shells are known from industry experience to be a result of manufacturing imperfections. These lead to maintenance requirements significantly before the 20-year design life [7, 8]. The high loss of earnings due to turbine standstill during blade replacement and repairs fuels the need for effective repair methods for a quick return to service.

The mechanical property restoration of scarf joints has been studied in the context of FRP, including the effect of the scarf ratio and external reinforcement plies [9-13]. A 1:50 scarf ratio has been shown in literature as well as practice to be a good compromise between restored mechanical properties and the size of the repair area [2]. Most work to-date has focused on the quasi-static or cyclic tensile loading effects of the scarf joint structure. Less studied are the fully-reversed cyclic fatigue behavior of the scarf joint structure for FRP. There is also a need for a systematic comparison of a large-to-small versus small-to-large layup. This work therefore aims to characterize the fully-reversed cyclic fatigue behavior of a 1:50 scarf joint structure depending on repair layup using representative glass FRP (GFRP) structures for wind turbine blade shell repair applications.

  doi:10.5075/epfl-298799_978-2-9701614-0-0

Methodology

2.1 Specimen Production

To examine the effect of the layup on the mechanical behavior of scarf joint structures, monolithic GFRP specimens were used in this study to isolate the joint interface region of interest. Representative of a portion of a scarf repair in the outer face sheet of a rotor blade shell, the specimens were produced using E-glass non-crimp fabric (NCF). Using the vacuum-assisted resin infusion (VARI) process with the RIMR135/RIMH137 and LR285/LH287 epoxy resin systems for the parent and repair sides, respectively, specimens were produced following the methodology described in [13]. A wet-to-hard layup was used to create the bi-material joint specimens, representative of wind turbine blade shell repairs in terms of materials and methods. Two repair layups were the focus of this work: large-to-small (LS) and small-to-large (SL). A detailed description of these two layups is given in [13].

Four groups of BIAX ±45° specimens were tested under quasi-static tensile load, as well as fully-reversed cyclic fatigue load under a range of load levels corresponding to the strains endured in-service by the blade shell: $\varepsilon_{\mathrm{x},0} = 0.2\%$ under rated wind and $\varepsilon_{\mathrm{x},0} = 0.5\%$ under 50-year gust loads [14]. Table 1 summarizes the specimen groups, including the terminology for group names used throughout this work, as well as the materials, repair layup, and fatigue load levels tested. The average fiber volume content of the parent material of the specimens was $V_{\mathrm{f}} = 0.46$, while the repair material side was $V_{\mathrm{f}} = 0.45$, determined according to Test Method I of ASTM D 3171-99:2000, Procedure G.

Table 1: Group parameters of tested GFRP coupon specimens.

Group name	Material	Sequence	Repair layup	Load levels tested
Parent reference	778 g/m^2 BIAX E-glass	$[\pm45°]_{4S}$	--	$\varepsilon_{x,0}$=0.2-0.4%
Repair reference	444 g/m^2 BIAX E-glass	$[\pm45°]_{4S}$	--	$\varepsilon_{x,0}$=0.3-0.5%
LS joint	778 g/m^2 BIAX E-glass + 444 g/m^2 BIAX E-glass	$[\pm45°]_{4S}$ + $[\pm45°]_{8S}$	Large-to-small	$\varepsilon_{x,0}$=0.25-0.4%
SL joint	778 g/m^2 BIAX E-glass + 444 g/m^2 BIAX E-glass	$[\pm45°]_{4S}$ + $[\pm45°]_{8S}$	Small-to-large	$\varepsilon_{x,0}$=0.25-0.4%

2.2 Test Parameters

The specimens were subjected to quasi-static tensile load according to DIN 527-1:2012-06 at a crosshead displacement speed of 2 mm/min, as well as fully-reversed (with load ratio $R = \frac{\sigma_{min}}{\sigma_{max}} = -1$) mechanical cyclic load on a 63 kN capacity Schenk PSB servo-hydraulic testing machine with hydraulic grips. Specimens were supported with an anti-buckling support to discourage unwanted displacement in the specimen thickness direction during the compressive component of the cyclic loading. All testing was done at room temperature. The number of cycles to failure was used as a metric to study the effect of the scarf joint layup on the cyclic

  doi:10.5075/epfl-298799_978-2-9701614-0-0

fatigue behavior of the structure, and testing frequency was varied across load levels to account for constant energy dissipation [15, 16]:

$$f = f_{ref}\left(\frac{\varepsilon_{ref}}{\varepsilon}\right)^2 \quad (1)$$

2. Results and Discussion

3.1 Quasi-static Tensile Loading

All groups of specimens were first subjected to quasi-static tensile load to understand the effect of the scarf joint layup on the restored tensile strength of the structure. The average ultimate tensile strength σ_{UTS} of all reference and joint specimens were compared and summarized in Table 2. Here, the restored values were calculated as a comparison of the average σ_{UTS} ultimate tensile strength of the joint group divided by the reference parent group:

$$\sigma_{\mathrm{UTS,restored}} = \frac{\sigma_{\mathrm{UTS,joint}}}{\sigma_{\mathrm{UTS,refence}}} \quad (2)$$

There was an overall high ultimate tensile strength σ_{UTS} restoration of the joint specimens, reaching a minimum of 80% for both layups, consistent with findings in literature for scarf joint structures [6, 17, 18]. In these specimens, the flat angle of the 1:50 scarf ratio connecting the two materials led to a high-quality joint. Both the reference and joint specimens failed due to intralaminar crack propagation through the specimen thickness. There was no significant change in failure mechanism caused by the presence of the LS joint, as discussed in [13], and the effect of the SL joint on the local failure mechanism was not detrimental to the restored strength due to the lack of change in global failure mechanism.

Prior to ultimate failure, the LS joint specimens underwent a period of localized necking in the specimen center before fracture, which had also been observed in ±45° FRP specimens without scarf joints subjected to tensile load. This was likely due to the concentration of IFF already having occurred in this region, making the material less stiff and thereby undergoing more local deformation.

Under quasi-static tensile load, the role of the SL joint on the restored ultimate tensile strength σ_{UTS} of the structure was relatively insignificant. Existing resin pockets in the joint interface served as localized damage initiation sites, which coalesced and led to ultimate failure with an intralaminar failure path. In comparison to the LS joint specimens, however, the fracture surface of the SL joint was larger due to the less localized behavior prior to fracture. The localized yielding of the resin pockets in the SL joint layup had a beneficial effect of breaking the fracture path, seen in Figure 1 with the relatively larger fracture surface in comparison to the LS joint specimen and in Table 2 with the higher restored σ_{UTS}.

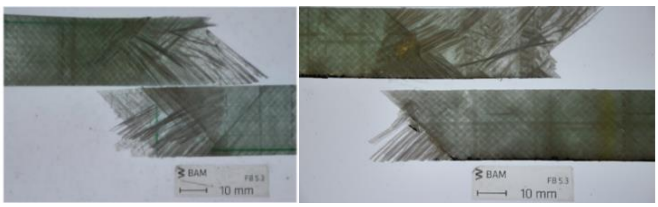

(a) LS joint (b) SL joint

Figure 1. Fractured surfaces of scarf joint specimens under quasi-static tensile load.

  doi:10.5075/epfl-298799_978-2-9701614-0-0

Table 2: Comparison of restored ultimate tensile strength σ_{UTS} between reference and joint specimens.

Group name	$\sigma_{\mathrm{UTS}} \pm S_{\mathrm{UTS}}$ / MPa	Restored σ_{UTS}
Parent reference	125 ±12	--
Repair reference	145 ±12	--
LS joint	100 ±25	0.80
SL joint	136 ±6	1.09

3.2 Cyclic Fatigue Loading

Upon understanding the quasi-static tensile behavior of the two scarf joint layups in comparison to the reference structure, all specimen groups were then subjected to fully-reversed cyclic fatigue loading. Fatigue behavior was summarized by plotting the number of cycles to failure N_{B} versus stress amplitude σ_{a} according to load level following DIN 50100:2016-12 and DIN SPEC 16457:2019-12, fit with the pearl string method as a power law fit derived from the Basquin equation [19]:

$$logN = a + b \cdot \log[\sigma_{\mathrm{a}}(N)] \tag{3}$$

The resulting S-N curve is shown in Figure 2. Fracture was taken as the failure criteria, and run-outs are marked with an outline and arrow. Both joint specimen groups failed in the parent region, speaking with adherend failure for the effectiveness of a 1:50 scarf joint.

Table 3 shows the average cycles to failure $N_{50\%}$of all test groups tested at a load level corresponding to $\varepsilon_{\mathrm{x},0} = 0.4\%$. This load level was chosen for comparison because all specimen groups were tested to failure, with no run-outs. The $N_{50\%}$ value of each joint group was compared to the parent reference group. For this, the restored fatigue strength was defined as:

$$N_{50\%,\mathrm{restored}} = \frac{N_{50\%,\mathrm{joint}}}{N_{50\%,\mathrm{parent}}} \tag{4}$$

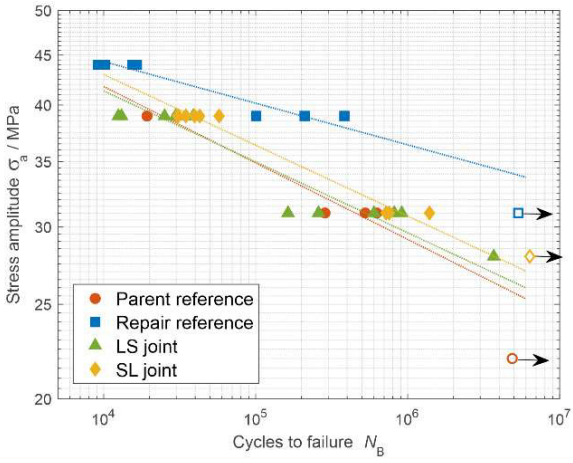

Figure 2. Fatigue behavior of all test groups, shown with a power law fit. Run-outs are marked with an outline and arrow.

The LS joint specimens consistently had a very similar cyclic fatigue strength to the parent reference groups across all tested load levels, as seen for the exemplary $\varepsilon_{x,0} = 0.4\%$ load level in Table 3. The effectiveness of the 1:50 scarf joint ratio allowed for a smooth load transfer between parent and repair adherends. The LS joint applied to a BIAX ±45° laminate, where fiber orientation mismatch insignificant in comparison to the applied load direction [13], was successful enough to not decrease the number of cycles to failure in the structure despite the disruption in continuous fiber reinforcement.

The SL joint specimens consistently had the highest restored fatigue strength across all load levels. As in the LS joint specimens, failure occurred in the parent adherend, speaking for the effectiveness of the scarf joint due to a good load transfer through shear stresses parallel to the scarf and thereby almost parallel to the load direction in the case of a flat angle. The resin pockets which result from the end of the repair layers in the joint interface seemed to act as a disruption to the damage propagation directly along the joint.

Table 3: Average cycles to failure $N_{50\%}$ of all joint specimens compared to reference specimens, tested at a load level corresponding to $\varepsilon_{x,0} = 0.4\%$.

Group name	$N_{50\%}$	$N_{50\%,\text{restored}}$
Parent reference	24167	--
Repair reference	200830	--
LS joint	23396	0.97
SL joint	38361	1.59

4. Conclusions

The failure of large-to-small and small-to-large scarf joint layups was examined under fully-reversed $R = -1$ cyclic load with GFRP coupon specimens. With a constant 1:50 scarf ratio, focus was directed to the influence of the joint interface variables and adherends on the cyclic fatigue behavior of the structure.

The effectiveness of the 1:50 scarf ratio and the low fiber orientation mismatch in a BIAX ±45° structure led to a successful load transfer across the joint in a large-to-small layup, and therefore a restored average cycles to failure $N_{50\%}$ similar to the reference parent structure. The resin pockets in the small-to-large layup did not play a detrimental role to the quasi-static and cyclic fatigue behavior of the scarf joint structure. By disrupting the damage propagation path combined with the fatigue-superior repair material, the SL joint structure had the highest restored average cycles to failure $N_{50\%}$.

Acknowledgements

This research was supported by funding from the Technical University of Berlin Manfred Fricke Foundation. The materials used for the experiments were made possible through the support of Saertex for the glass non-crimp fabrics and Hexion for the epoxy resins and hardeners. The

  doi:10.5075/epfl-298799_978-2-9701614-0-0

authors would also like to acknowledge Stefan Hickmann, Nicolai Schmidt, and Julian Marzik for their support in specimen production and test setup.

5. References

1. Cardrick A and Smith M. An approach to the development of meaningful design rules for fatigue-loaded CFRP components, Composites 1974; 96-100.

2. Lekou D and van Wingerde A. Evaluation of Repair Techniques as Used for Small Specimens. Optimat Blades Technical Report 2006.

3. Oztelcan C, Ochoa O, Martin J, Sem K. Design and analysis of test coupons for composite blade repairs, Composite Structures 1997; 37:185-193.

4. Caminero M, Pavlopoulou S, Lopez-Pedrosa M, Nicolaisson B, Pinna C, Soutis C. Analysis of adhesively bonded repairs in composites: Damage detection and prognosis, Composite Structures 2013; 95:500-517.

5. Jen Y-M. Fatigue life evaluation of adhesively bonded scarf joints, International Journal of Fatigue 2012; 36:30-39.

6. Lekou D and Vionis P. Report on repair techniques for composite parts of wind turbine blades. Optimat Blades Technical Report 2002.

7. Trappe V and Nielow D. Fatigue loading of sandwich shell test specimens with simulated production imperfections and in-situ NDT, in ICFC 7 – The International Conference on Fatigue of Composites 2018.

8. Nielow D. Einfluss fertigungsbedingter Imperfektionen auf die Betriebsfestigkeit von FKV-Schalenstrukturen in Sandwichbauweise, Technische Universität Dresden 2022.

9. Moreira R, De Moura M, Silva F, Ramirez F. Numerical comparison of several composite bonded repairs under fatigue loading, Composite Structures 2020; 243.

10. Ahn S and Springer G. Repair of composite laminates – I: Test results, Journal of Composite Materials 1998; 32:1036-1074.

11. Yoo J-S, Truong V-H, Park M-Y, Choi J-H, Kweon J-H. Parametric study on static and fatigue strength recovery of scarf-patch-repaired composite laminates, Composite Structures 2016; 140:417-432.

12. Wu C, Chen C, He L, Yan W. Comparison on damage tolerance of scarf and stepped-lap bonded composite joints under quasi-static loading, Composites Part B: Engineering 2018; 155:19-30.

13. Ghafafian C, Popiela B, Trappe V. Failure Mechanisms of GFRP Scarf Joints under Static Tensile Load, Materials 2021; 14.

14. Grasse F. Beitrag zur Untersuchung des Betriebsfestigkeitsverhaltens von Rotorblättern für Windenergieanlagen im verkleinerten Maßstab, Technische Universität Berlin 2014.

15. Trappe V. Beschreibung des intralaminaren Ermüdungsverhaltens von CFK mit Hilfe innerer Zustandsvariablen, Technische Universität Carolo-Wilhelmina Braunschweig 2001.

  doi:10.5075/epfl-298799_978-2-9701614-0-0

16. Krause O. Frequency effects on lifetime, DLR Technical Report 2002.

17. Kumari P, Wang J, Sahil. Residual Tensile Strength of the Multi-impacted Scarf-repaired Glass Fiber-reinforced Polymer (GFRP) Composites, Materials 2018; 11.

18. Jen Y-M and Ko C-W. Evaluation of fatigue life of adhesively bonded aluminum single-lap joints using interfacial parameters, International Journal of Fatigue 2009; 32:330-340.

19. Basquin O. The exponential law of endurance tests, in American Society for Testing and Materials Proceedings 1910.

  doi:10.5075/epfl-298799_978-2-9701614-0-0